Time dependent ratcheting-fatigue interactions of tempered 42CrMo steel: Experiments and constitutive model

Juan Zhang*, Haibo Luo, Guozheng Kang, Qianhua Kan

School of Mechanics and Engineering, Southwest Jiaotong University, Chengdu 610031, PR China
* Corresponding author: sarazj@126.com

Abstract The time dependent ratcheting behavior and fatigue failure, as well as their interaction were investigated by uniaxial cyclic stressing tests for tempered 42CrMo steel at room temperature. The effects of stress rates and peak stress hold on the ratcheting strain and final failure life were discussed. Then based on the experimental observations, a damage-coupled constitutive model was developed to simulate the whole-life ratcheting by employing a static recovery term in the nonlinear kinematic hardening rule. Comparing with the corresponding experimental results, it is shown that the developed model can describe the whole-life ratcheting behavior of the tempered 42CrMo steel reasonably.

Keywords Ratcheting, Low-cycle fatigue, Visco-plastic constitutive model, Damage, Tempered 42CrMo steel

1. Introduction

When the materials and structures are subjected to a stress-controlled cyclic loading with non-zero mean stress, ratcheting, a cyclic accumulation of inelastic deformation, will occur. Since ratcheting is a secondary deformation superposed on the primary cyclic stress–strain response and develops progressively during the cyclic loading, it is very important and should be addressed in the safety assessment and fatigue life estimation of the materials and structure components. Therefore, the ratcheting has been extensively studied in the last twenty years and many cyclic constitutive models were established to describe the ratcheting[1-8]. However, the referable literature focused mainly on the ratcheting deformation and its constitutive modeling, and the whole-life ratcheting and fatigue failure life were not addressed, since the number of applied cycles was relatively small there. The models do not consider any effect of fatigue damage on the ratcheting, and fail to simulate the whole-life ratcheting of the materials. It is necessary to discuss the ratcheting–fatigue interaction and simulate the whole-life ratcheting and fatigue failure life of the materials.

The low-cycle fatigue involving the ratcheting, i.e., ratcheting–fatigue interaction[9-11] has been investigated recently by some researchers due to its significance in the design and assessment of structure components. And a damage-coupled cyclic constitutive model was constructed by Kang et al.[12] to describe the whole-life ratcheting and predicting the failure life of the materials. It is proved that the simulated whole-life ratcheting behavior and predicted failure life of tempered 42CrMo steel are in a fairly good agreement with the experimental ones. However, the effects of some time-related factors, such as stress rate, hold-time, and so on, on the ratcheting behavior and fatigue failure are not involved in the referable literature. So in this work, the time dependent ratcheting behavior and fatigue failure, as well as their interaction were investigated. Firstly, the ratcheting behavior and low-cycle fatigue for tempered 42CrMo steel were investigated by uniaxial cyclic stressing tests at room temperature. The effects of stress rates and peak stress hold on the ratcheting strain and final failure life were discussed. Then based on the experimental observations, a damage-coupled constitutive model was developed to simulate the whole-life ratcheting by employing a static recovery term in the nonlinear kinematic hardening rule.

2. Experimental results and discussions

The material used in this work is 42CrMo steel. Its chemical composition is: C, 0.43%; Mn, 0.68%; Si, 0.27%; P, 0.014%; Cr, 1.11%; Ni, 0.05%; W, 0.01%; Mo, 0.17%; V, 0.01%; Ti, 0.004%; Cu, 0.03%; Fe, remained. The as-forged 42CrMo steel bars were tempered (tempering at 560℃ after heating at 850℃ for 1h and quenching in oil), and then were machined to be round, solid bar fatigue specimens with test section diameter of 10mm and gauge length of 30mm for uniaxial tests. The test machine was MTS809-250KN; the loading process was controlled and the experimental data were collected by Teststar control system attached to the machine. The axial strain was measured by a tensile extensometer, whose limited axial nominal strain was 50%. The specimens were tested under monotonic tension, uniaxial cyclic straining and uniaxial cyclic stressing at room temperature. To illustrate the ratcheting behavior more clearly, the variation of ratcheting strain ε_{r} (defined by Eq. (1)) with the number of cycles for each loading case of cyclic stressing, was obtained from the experimental data and is shown in the figures in this section. In this work, the ratcheting strain ε_{r} is defined as

$$\varepsilon_{\mathrm{r}} = \frac{1}{2}\left(\varepsilon_{\max} + \varepsilon_{\min}\right) \tag{1}$$

where $\varepsilon_{\max}$ is the maximum axial nominal strain in each cycle measured by the extensometer, and $\varepsilon_{\min}$ is the minimum. Meanwhile, in this work, the ratcheting true strain rate is defined as the increment of ratcheting strain after each cycle and denoted as $\mathrm{d}\varepsilon_{\mathrm{r}}/\mathrm{d}N$, where *N* means the number of cycles.

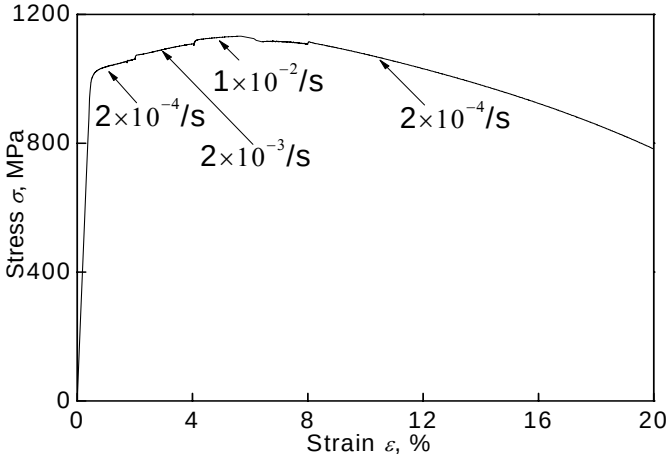

Figure 1. Monotonic tensile stress-strain curves with different straining rates

Monotonic tensile results of tempered 42CrMo steel at different straining rates are shown in Fig. 1. It is shown that the material exhibits rate-dependence at room temperature, and the responded stress at smaller strain rate is much lower than that at higher one.

2.1. Time-dependent strain cyclic features

The cyclic softening/hardening features of the material were investigated under the symmetrical axial cyclic straining (±0.6%) at different straining rates (0.2%/s and 0.04%/s). It can be seen from Fig. 2 that: (1) the material presents significant cyclic at two straining rates, (2) the cyclic softening behavior of the material is rate-dependent even at room temperature, i.e., responded stress amplitude at smaller straining rate is lower than that at higher one.

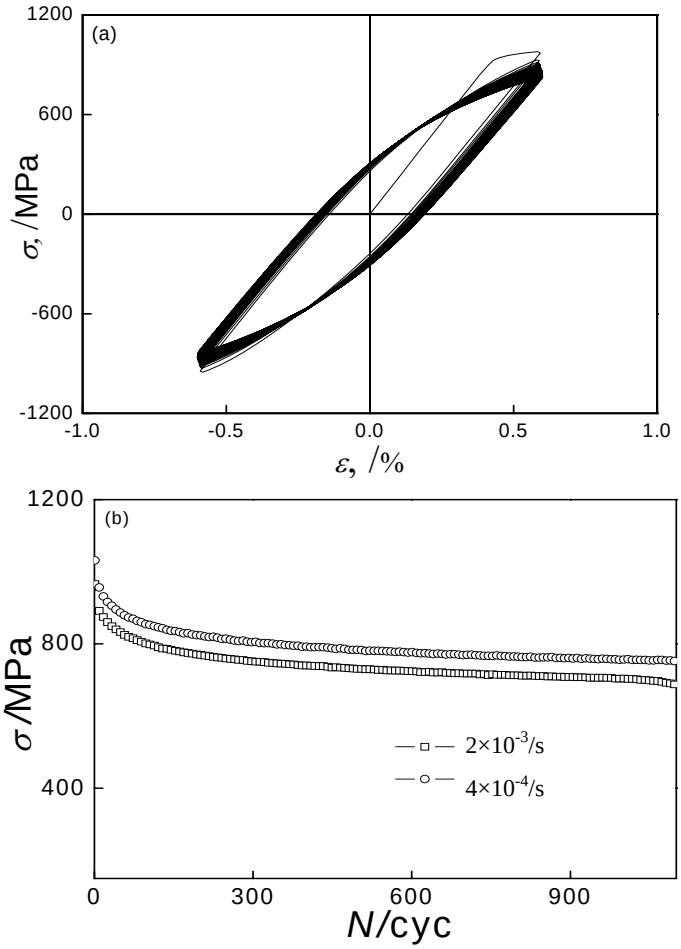

Figure 2. Results of symmetrical axial cyclic straining at different straining rates: (a) stress–strain curve at straining rate of 0.2%/s; (b) curves of stress amplitude vs. cyclic number at two straining rates

2.2. Time-dependent ratcheting-fatigue interactions

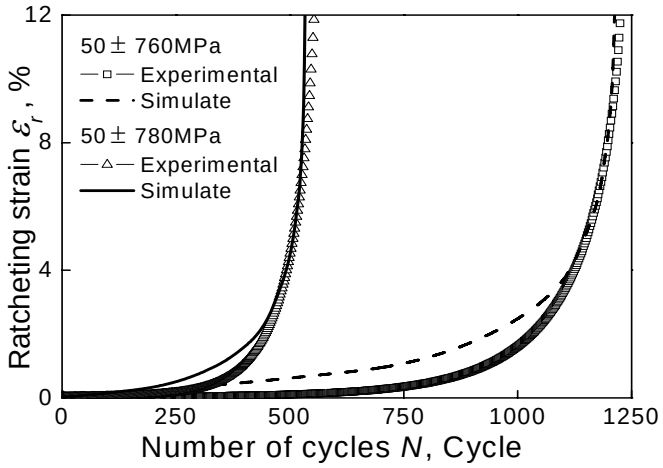

Figure 3. Experimental and simulated whole life ratcheting with different stress amplitude

Firstly, the specimens were tested by cyclic stressing with various nominal stress amplitudes, mean nominal stresses at the same stress rate till the failure occurred. The experimental results of ratcheting behavior of tempered 42CrMo steel at room temperature (shown in Fig.3 and Fig.4) is the same as that was observed in previous work[11]: (1) The evolution of ratcheting strain can be

divided as three stages regarding to the different ratcheting strain rates due to the cyclic softening feature of tempered 42CrMo steel, i.e., the first stage with decreasing ratcheting strain rate, the second stage with an almost constant rate and the third stage with quickly increasing rate. (2)When the stress amplitude or mean stress increases, the ratcheting strain ε_r increases correspondingly, and the first and second stages are ended and the third stage appears more quickly, causing the failure of the material within fewer cycles.

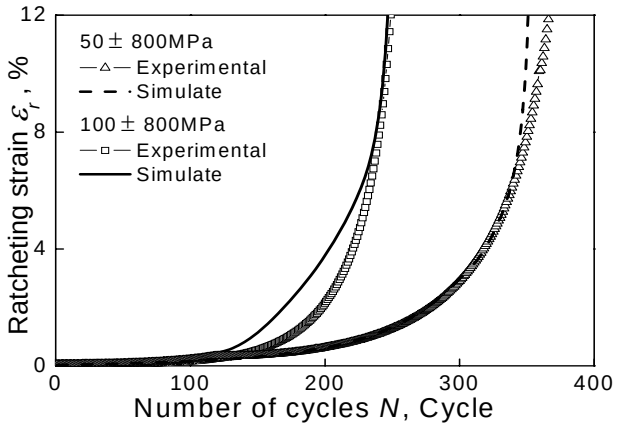

Figure 4. Experimental and simulated whole life ratcheting with different mean stress

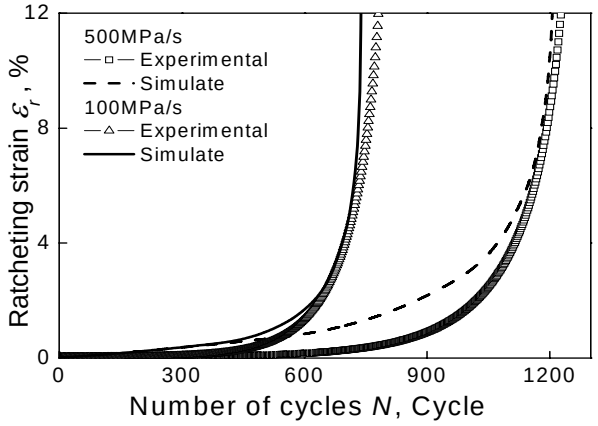

Figure 5. Experimental and simulated whole life ratcheting at different stress rate

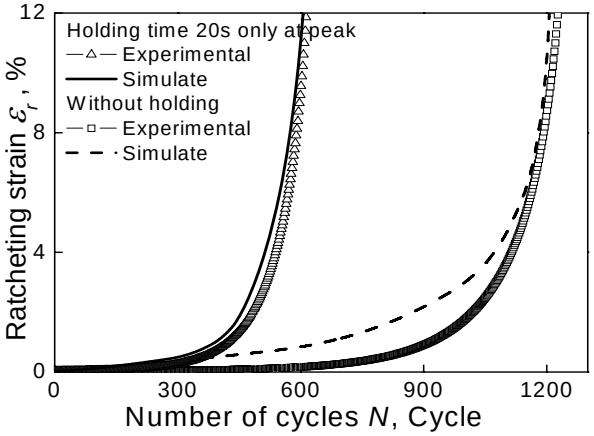

Figure 6. Experimental and simulated whole life ratcheting with and without peak stress holding time

Then the axial cyclic stressing tests were done with constant mean stress and stress amplitude (50 ± 760MPa) but at different stress rates (500 and 100MPa/s). The experimental result is shown in Fig.5. It can be seen that the effect of stressing rate on the ratcheting and fatigue life is remarkable. The evolution of ratcheting strain also can be divided as three stages at different stress rates, but the ratcheting strain ε_r increases with the increasing of stress rate, and the first and second stages are ended and the third stage appears more quickly at lower stress rate, causing the failure of the material within fewer cycles.

The effect of the peak stress hold in each cycle on ratcheting and fatigue life also was discussed under uni-stepped axial cyclic stressing test (50 ± 760MPa) at stressing rate of 500MPa/s. It is concluded from Fig. 6 that non-zero hold-time influences apparently the ratcheting and the fatigue life of the material. The ratcheting strain ε_r with peak stress holding is larger than that without peak stress holding. When the stress holds 20s at peak, the first and second stages of ratcheting are ended and the third stage appears more quickly, so the material fails within fewer cycles

3. Constitutive model and simulation

To describe the ratcheting–fatigue interaction of the tempered 42CrMo steel, Kang et al.[12] proposed a damage-coupled visco-plastic cyclic constitutive model. It has been verified their model could simulate the whole-life ratcheting and predict the fatigue failure life of the material reasonably. So in this work，the damage-coupled visco-plastic cyclic constitutive model proposed by Kang was used to describe the whole-life ratcheting of the material, except that a new nonlinear kinematic hardening rule was introduced to improve the description of time-dependent ratcheting behavior.

3.1. Damage-coupled constitutive model

The governing equations of the damage-coupled constitutive model are outlined as follows:

$$\varepsilon_{ij} = \varepsilon_{ij}^{e} + \varepsilon_{ij}^{vp} \tag{2}$$

$$\varepsilon_{ij}^{e} = \frac{1+\nu}{E}\left(\frac{\sigma_{ij}}{1-D}\right) - \frac{\nu}{E}\left(\frac{\sigma_{kk}\delta_{ij}}{1-D}\right) \tag{3}$$

$$\dot{\varepsilon}_{ij}^{vp} = \frac{3}{2}\frac{\dfrac{S_{ij}}{1-D} - \alpha_{ij}}{\left(\dfrac{S_{ij}}{1-D} - \alpha_{ij}\right)_{eq}}\left(\frac{\dot{\lambda}}{1-D}\right) \tag{4}$$

$$F_y = \left(\frac{S_{ij}}{1-D} - \alpha_{ij}\right)_{eq} - Q \tag{5}$$

$$\frac{\dot{\lambda}}{1-D} = \dot{p} = \left\langle \frac{F_y}{K} \right\rangle^{n} \tag{6}$$

$$\left(\frac{S_{ij}}{1-D}-\alpha_{ij}\right)_{eq}=\sqrt{\frac{3}{2}\left(\frac{S_{ij}}{1-D}-\alpha_{ij}\right)\left(\frac{S_{ij}}{1-D}-\alpha_{ij}\right)} \quad (7)$$

In previous work[13], a new kinematic hardening rule with a static recovery term (based on the Ohno–Abdel-Karim equation[5]) provide a reasonable simulation to the time-dependent ratcheting of SS304 stainless steel. So in this work, the damage was introduced in the kinematic hardening rule with a static recovery term to describe the whole-life time-dependent ratcheting of tempered 42CrMo steel. The evolution law of nonlinear kinematic hardening rule is

$$\alpha_{ij}=\sum_{k=1}^{M}\alpha_{ij}^{(k)} \quad (8)$$

$$\dot{\alpha}_{ij}^{(k)}=\xi^{(k)}\left[\frac{2}{3}r^{(k)}(1-D)\dot{\varepsilon}_{ij}^{p}-\mu\alpha_{ij}^{(k)}\dot{\bar{\varepsilon}}^{p}-H(f^{(k)})(1-\mu)\alpha_{ij}^{(k)}\dot{\bar{\varepsilon}}^{p}\right]-\chi^{(k)}\left(\bar{\alpha}^{(k)}\right)^{m^{(k)}-1}\alpha_{ij}^{(k)} \quad (9)$$

The evolution law of isotropic hardening is

$$\dot{Q}=\gamma(Q_{\infty}-Q)\dot{\bar{\varepsilon}}^{p}=\gamma(Q_{\infty}-Q)\dot{p}(1-D) \quad (10)$$

In above equations, D is the damage variable. From the evolution feature of the damage during the stress cycling, it is concluded that the total damage presented in the stress cycling can be divided as two parts, i.e., elastic damage and plastic damage[12]:

$$D=D_{\mathrm{e}}+D_{\mathrm{p}} \quad (11)$$

The evolution rules of D_{e} and D_{p} are

$$\dot{D}_{e}=\left(\frac{\sigma_{eq}^{2}}{2E_{0}S_{e}(1-D)^{2}}\right)\dot{p} \quad (12)$$

$$\dot{D}_{p}=\left(\frac{\sigma_{eq}^{2}}{2E_{0}S_{p}(1-D_{p})^{2}}\right)\dot{p} \quad (13)$$

It can be seen that they have the same original form but different constants. When the plastic strain is very small, the macroscopic elastic damage is a main cause of the fatigue damage; however, when the plastic strain develops significantly due to the cyclic softening of the material, the plastic damage dominates the damage after certain cycles[12].

3.2. Simulations to whole life ratcheting

In the constitutive model, the material parameters relative to the evolution of elastic and plastic damages can be determined from the experimental results by the method mentioned in reference [12]. For simplicity, other material parameters are determined from the experiments without any fatigue damage considered. In this case, the procedure to determine the parameters is similar to that used by Kang[8]. The values of all material parameters used in the proposed damage-coupled constitutive model are listed in Table 1.

Table 1. Material parameters used in the constitutive model

M=10, E_0=213GPa, v=0.3, K=90MPa, n=10, Q_0=709.5MPa;
$\zeta^{(1)}=6060.6$， $\zeta^{(2)}=2020.2$， $\zeta^{(3)}=673.4$, $\zeta^{(4)}=303.3$, $\zeta^{(5)}=151.5$, $\zeta^{(6)}=75.7$, $\zeta^{(7)}=43.2$
$\zeta^{(8)}=28.8$， $\zeta^{(9)}=21.6$， $\zeta^{(10)}=17.3$； $r^{(1)}=203.5$， $r^{(2)}=26.4$, $r^{(3)}=13.6$, $r^{(4)}=1.8$, $r^{(5)}=2.1$,
$r^{(6)}=1.4$， $r^{(7)}=7.9$， $r^{(8)}=20.1$， $r^{(9)}=42.8$， $r^{(10)}=19.2$ (MPa);
$\gamma=0.2$， $\mu=0.15$， $Q_\infty=600$ MPa;
$\sigma_{-1}^{f}=419.6$ MPa, $A_1=7.4\times10^{-5}$， $A_2=2.2\times10^{-6}$， $A_3=8.16$， $A_4=-0.569$， $S_p=29$ MPa.

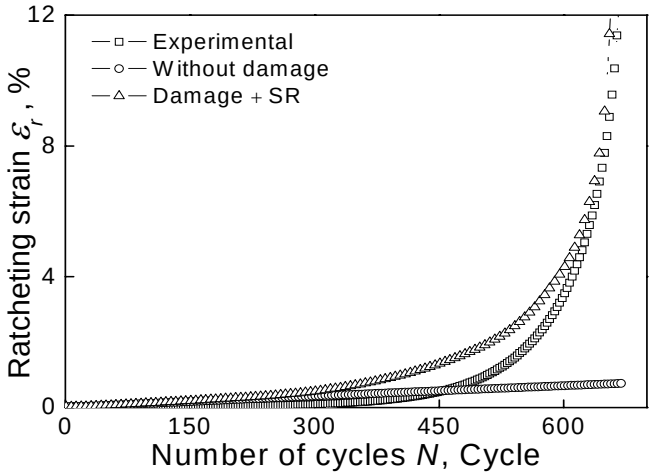

Figure 7. Experimental and simulated whole-life ratcheting by the model coupled with damage or not

The uniaxial whole-life time-dependent ratcheting behavior of tempered 42CrMo steel is simulated by the damage-coupled constitutive model. Fig. 7 shows the experimental and simulated results (50±780MPa, 500MPa/s) obtained by the damage-coupled model and the model with no damage, respectively. It is seen from Fig.7 that the constitutive model introducing damage gives a reasonable simulation for the whole-life ratcheting, especially for the accelerated increase of ratcheting strain at the end stage of cycling.

Figs. 3 and 4 provide some simulated results obtained by the model for some loading cases with various nominal stress amplitudes, mean nominal stresses at the same stress rate. It is shown that the simulated results are in fairly good agreement with the experimental ones and cyclic softening feature of the material on the ratcheting behavior are reasonably considered because of the introducing of damage.

Fig. 5 shows the simulated results of whole life ratcheting behavior at different stress rate, which loading condition is 50±760MPa. It is shown that the constitutive model proved good simulation to the effect of stress rate, and the ratcheting strain and ratcheting strain rate were increase with the decline of stress rate. Fig. 6 shows the simulated results of whole life ratcheting behavior with and without peak stress hold. It is shown that the simulated results are in fairly good agreement with the experimental ones. In one word, the developed constitutive model can describe the time dependent ratcheting reasonably since a static recovery term is introduced to the kinematic hardening rule.

4. Conclusions

(1) The tempered 42CrMo steel presents a rate-dependence under monotonic tension and uniaxial cyclic straining at room temperature. The variations of stress rate and peak stress hold-time have remarkable effect on the ratcheting behavior and low-cycle fatigue life.

(2) Based on the experimental results, a damage-coupled cyclic constitutive model is develops in the framework of continuum damage mechanics and unified visco-plasticity. In the model, the effects of cyclic softening feature and fatigue damage on the ratcheting are addressed by introducing the damage variable *D*. And the effects of stress rate and peak stress hold are simulated by employing a static recovery term in the nonlinear kinematic hardening rule. The model describes the whole-life ratcheting behavior of the material reasonably. The model describes the whole-life time dependent ratcheting behavior of the material reasonably.

Acknowledgements

The work was financially supported by the Fundamental Research Funds for the Central Universities (SWJTU11CX070).

References

[1] Chaboche, J.L., On some modifications of kinematic hardening to improve the description of ratcheting effects, Int. J. Plast., 7, (1991) 661–678.
[2] Ohno, N.,Wang, J.D., Kinematic hardening rules with critical state of dynamic recovery: I. Formulation and basic features for ratcheting behaviour, Int. J. Plast., 9, (1993)375–389.
[3] Ohno, N.,Wang, J.D., Kinematic hardening rules with critical state of dynamic recovery: II. Application to experiments of ratcheting behaviour, Int. J. Plast., 9, (1993) 390–403.
[4] Jiang, Y., Sehitoglu, H., Modeling of cyclic ratcheting plasticity, ASME J. Appl. Mech., 63, (1996) 720–733.
[5] Abdel-Karim, M., Ohno, N., Kinematic hardening model suitable for ratcheting with steady-state, Int. J. Plast., 16, (2000) 225–240.
[6] Bari, S., Hassan, T., An advancement in cyclic plasticity modeling for multiaxial ratcheting simulation, Int. J. Plast., 18, (2002) 873–894.
[7] Chen, X., Jiao, R., Modified kinematic hardening rule for multiaxial ratcheting prediction, Int. J. Plast., 20, (2004) 871–898.
[8] Kang, G.Z., A visco-plastic constitutive model for ratcheting of cyclically stable materials and its finite element implementation, Mech. Mater., 36, (2004) 299–312.
[9] Kwofie, S., Chandler, H.D., Low cycle fatigue under tensile mean stresses where cyclic life extension occurs, Int. J. Fatigue, 23, (2001) 341–345.
[10] Yang, X.J., Low cycle fatigue and cyclic stress ratcheting failure behavior of carbon steel 45 under uniaxial cyclic loading, Int. J. Fatigue, 27, (2005) 1124–1132.
[11] Kang, G.Z., Liu, Y.J., Uniaxial ratcheting and low-cycle fatigue failure of the steels with cyclic stabilizing or softening feature, Mater. Sci. Eng. A, 472 (1–2), (2008) 258–268.
[12] G.Z. Kang, Y.J. Liu, J. Ding, Q. Gao, Uniaxial ratcheting and fatigue failure of tempered 42CrMo steel: Damage evolution and damage-coupled visco-plastic constitutive model, Int. J. Plast., 25, (2009) 838–860.
[13] Q.H. Kan, G.Z. Kang, J. Zhang, Uniaxial time-dependent ratchetting: Visco-plastic model and finite element application, Theoretical and Applied Fracture Mechanics, 47, (2007) 133–144.